

A cyber-physical-social system with parallel learning for distributed energy management of a microgrid

Xiaoshun Zhang^{a,b}, Tao Yu^{b,*}, Zhao Xu^a

^a Department of Electrical Engineering, The Hong Kong Polytechnic University, Hong Kong

^b College of Electric Power, South China University of Technology, 510640 Guangzhou, China

Abstract—A novel cyber-physical-social system (CPSS) with parallel learning is presented for distributed energy management (DEM) of a microgrid. CPSS is developed by extending the conventional cyber-physical system to the social space with human participation and interaction. Each energy supplier or each energy demander is regarded as a human in the social space, who is able to learn the knowledge, cooperate with others, and make a decision with various preference behaviors. The correlated equilibrium (CE) based general-sum game is employed for realizing the human interaction on the complex optimization subtask, while the novel adaptive consensus algorithm is used for achieving that on the simple optimization subtask with multi-energy balance constraints. A real-world system and multiple virtual artificial systems are introduced for parallel and interactive execution based on the small world network, thus a higher quality optimum of DEM can be rapidly emerged with a high probability. Case studies of a microgrid with 11 energy suppliers and 7 energy demanders demonstrate that the proposed technique can effectively achieve the human-computer collaboration and rapidly obtain a higher quality optimum of DEM compared with other centralized heuristic algorithms.

Keywords – Cyber-physical-social system; Parallel learning; Correlated equilibrium; Adaptive consensus algorithm; Distributed energy management

* Corresponding author. Tel.: +86 13002088518.

E-mail address: taoyu1@scut.edu.cn (T. Yu).

Nomenclature			
<i>Variables</i>		$a^{\text{lin}}, b^{\text{lin}}$	coefficients of linear demand versus price expression
P_{dg}	electricity energy output of DG	N_{dg}	number of DG
H_{h}	heat energy output of heat-only unit	N_{h}	number of heat-only units
P_{chp}	electricity energy output of CHP unit	N_{chp}	number of CHP units
H_{chp}	heat energy output of CHP unit	N_{dr}	number of energy demanders
P_{tie}	tie-line power	N_{wt}	number of WT
ΔD	responding power	N_{pv}	number of PV units
a_j	action of the j th agent	η	maximum allowable power curtailment portion
Q_j^k	the knowledge matrix of the j th agent	α	knowledge learning factor
π_j	probability distributions of state-action pairs	γ	discount factor
R_j	feedback reward of the j th agent	ε	exploitation rate
λ_p	incremental cost of the p th agent	μ	adjustment factor of energy mismatch
x_j^k	solution of the j th agent at the k th iteration	C_1, C_2	feedback reward coefficients
x_p^c	energy consensus value of the p th agent	k_{max}	maximal iteration number
x^{ik}	current solution of the i th VAS	<i>Abbreviations</i>	
x_b^{rk}	current best solution of the real-world system	CE	correlated equilibrium
p_{iw}	interaction probability between the i th VAS and the w th VAR	CPS	cyber-physical system
h^i	current best VAS in the i th VAR's interactive network	CPSS	cyber-physical-social system
f_{cost}	total operating cost	DERs	distributed energy resources
v	current wind speed	EMS	energy management system
S	current irradiance	DEM	distributed energy management
T	ambient temperature	RL	reinforcement learning
<i>Parameters</i>		DG	diesel generator
v_r	rated wind speed	VASs	virtual artificial systems
$v_{\text{in}}, v_{\text{out}}$	cut-in and cut-out wind speeds	WT	wind turbine
α_{pv}	temperature coefficient	PV	photovoltaic
$\alpha_{\text{dg}}, \beta_{\text{dg}}, \gamma_{\text{dg}}$	fuel cost coefficients of DG	CHP	combined heat and power
$\alpha_{\text{h}}, \beta_{\text{h}}, \gamma_{\text{h}}$	operating cost coefficients of heat-only unit	GA	genetic algorithm
$\alpha_{\text{chp}}, \beta_{\text{chp}}, \gamma_{\text{chp}}$	operating cost coefficients of CHP unit	PSO	particle swarm optimization
$\delta_{\text{chp}}, \theta_{\text{chp}}, \zeta_{\text{chp}}$	operating cost coefficients of CHP unit	ABC	artificial bee colony
$C_{\text{buy}}, C_{\text{sell}}$	electricity buying price and selling price	GSO	group search optimizer

1. Introduction

With the rapid development of increasing renewable energy, the energy internet [1] which aims to realize the coordination among various generations, storage devices, and loads in a wide area by the internet technology, has gained extensive studies in recent years [2]. At present, energy internet is essentially a tight integration between cyber and physical resources, i.e., an application of cyber-physical system (CPS) on integrated energy systems [3]. Although CPS [4] can offer many potential benefits to the energy internet, including faster response, higher control precision, larger scale distributed coordination, and so on, but it almost ignores the human participation and interaction. In fact, the energy internet is highly coupled with the human and social characteristics [5], thus CPS may not satisfy different optimal operations of integrated energy systems in some cases, e.g., the demand response management without considering the social characteristics of different consumers. As a result, the cyber-physical-social system (CPSS) [6] was developed by logically extending CPS to the social space with human participation and interaction. As a promising system architecture of industry, CPSS is well available as a core part of future intelligent energy systems [7], rightfully including the multi-energy microgrid.

Microgrid is usually a small-scale multi-energy system with a low-voltage distribution network [8], which can effectively integrate various distributed energy resources (DERs), storage devices, and controllable loads in the grid-connected or islanded mode. In general, energy management of a microgrid seeks to minimize the total operating cost via an optimal dispatch strategy of energy balance among DERs, storage devices, tie-line power from the main grid, and controllable loads under various constraints [9]. In order to address this problem, the centralized optimization is the most commonly used type of methods, e.g., mixed integer linear programming [10] and gravitational search algorithm [11], which often produce a satisfactory result with a low total operating cost. However, it easily leads to a communication bottleneck in a microgrid with a larger number of controllable devices since the centralized energy management systems (EMS) needs to collect and process all the corresponding information from each one, which also cannot ensure the security and privacy of each owner [12]. In terms of the optimization performance, the centralized optimizer is apt to trap in a relatively high computation burden or a low-quality optimum with the great increasing controllable devices. Furthermore, it cannot satisfy the requirement of high operation reliability because the operation of an entire microgrid completely depends on the only centralized optimizer.

For the sake of handling these issues, the distributed control architecture is more suitable for the practical energy management [13], thus various distributed optimization algorithms have been proposed for distributed energy management (DEM) of a microgrid. The consensus algorithms have been deeply researched for DEM due to its remarkable self-organizing ability, significant robustness, and easy scalability [14]-[16], in which the performance influence by the time delays in communication network is strictly investigated in [17]. Besides, the subgradient based distributed optimization was also successfully designed for minimizing the total operating cost of a microgrid [18],[19]. In order to effectively realize the complex interaction among independent agents [20], the game theory, e.g., Stackelberg game [21] and bargaining game [22], were introduced to combine different optimization techniques for DEM. Unfortunately, all of these algorithms mainly suffer from the following four problems:

- High independence on the mathematical model*: The core optimizers are essentially the gradient-based algorithms, the performance of which are fully determined by the initial solution of DEM. Therefore, it easily leads to a low quality local-optimum if nonlinearities, nonconvexity, discontinuous and nondifferentiable objective functions (e.g., purchase energy cost or sell energy benefit according to direction of tie-line power), and complex constraints (e.g, the heat-power feasible operation region of combined heat and power (CHP) units [23]) exist.

- Incapability of knowledge learning and single decision strategy*: Each game agent is constructed with only a single decision strategy and is incapable of knowledge learning, which is not consistent with the intelligent human in real-world system.

- Invalid multi-energy interactions with consensus algorithm*: The consensus based human interaction is only suitable for

only single energy interaction among the local energy supplier and demander, which cannot satisfy the multi-energy interaction with multiple energy balance constraints.

●*Inefficient optimization with a single execution system*: The traditional game theory based human interaction usually seeks an optimal equilibrium with a single execution system, which easily results in a long computation time as the iterations may involve repeated games.

In order to simultaneously address these problems, this paper proposes a CPSS with parallel learning for DEM of a microgrid, which has the following features and novelties:

- CPSS is firstly introduced to DEM of a microgrid, which fully considers the human (energy supplier or energy demander) participation and interaction, thus the obtained dispatch strategy is more practical for an optimal operation.
- The model-free Q-learning can effectively enable each agent to flexibly handle the nonconvex nonlinear DEM with complex constraints and nondifferentiable objective functions, while each agent can learn the knowledge from the continuous interactions with the environment. Instead of a single decision strategy, the correlated equilibrium (CE) based general-sum game [24] with multiple decision strategies is used for increasing the decision diversity of each human.
- By improving the original consensus algorithm, the adaptive consensus algorithm is proposed for effectively achieving the multi-energy interactions with multiple energy balance constraints, thus they can reach a consensus (optimum) on the incremental cost.
- Multiple virtual artificial systems (VASs) are built to guide the real-world system for DEM with a single execution system, thus the game interaction efficiency of the real-world system can be dramatically improved without any adverse trials according to the guidance by all the VASs. Besides, the small world network is adopted for constructing the interaction network among different VASs, which can properly balance the exploitation and exploration of VASs.

The remaining of this paper is organized as follows. Section 2 presents the mathematical model of DEM of a microgrid. Section 3 gives the design of CPSS with parallel learning for DEM. Case studies are carried out in Section 4. Finally, Section 5 concludes the paper.

2. Mathematical model of DEM of a microgrid

2.1. Energy suppliers

(i) *Renewable energy resources*: for improving the generation power outputs of renewable energy resources, both the wind turbine (WT) and photovoltaic (PV) unit are operated at the maximum power points under different weather conditions, which can be expressed as follows [25],[26]:

$$P_{wt} = \begin{cases} 0, & \text{for } v < v_{in} \text{ and } v > v_{out} \\ P_{wt}^r \frac{v - v_{in}}{v_r - v_{in}}, & \text{for } v_{in} \leq v \leq v_r \\ P_{wt}^r, & \text{for } v_r < v \leq v_{out} \end{cases} \quad (1)$$

$$P_{pv} = P_{pv}^r (1 + \alpha_{pv} \cdot (T - T_{ref})) \cdot \frac{S}{1000} \quad (2)$$

where P_{wt} and P_{pv} are the current maximum power points of WT and PV unit, respectively; P_{wt}^r and P_{pv}^r are the rated power of WT and PV unit, respectively; v_r is the rated wind speed; v is the current wind speed; v_{in} and v_{out} are the cut-in and cut-out wind speeds, respectively; S is the current irradiance; T is the ambient temperature; T_{ref} is the reference temperature; and α_{pv} is the temperature coefficient.

(ii) *Diesel generator*: as a common DER, the fuel cost of diesel generator (DG) can be expressed via a quadratic function, as follows [27]:

$$f_{dg}(P_{dg}) = \alpha_{dg} + \beta_{dg} P_{dg} + \gamma_{dg} P_{dg}^2 \quad (3)$$

where P_{dg} is the electricity energy output of DG; α_{dg} , β_{dg} , and γ_{dg} are the fuel cost coefficients of DG.

(iii) *Heat-only unit*: such as gas furnace or heater exchanger, it can only provide the heat energy for local demanders in a microgrid. Similarly, its operating cost can be constructed as a quadratic function, as follows [27]:

$$f_h(H_h) = \alpha_h + \beta_h H_h + \gamma_h H_h^2 \quad (4)$$

where H_h is the heat energy output of heat-only unit; α_h , β_h , and γ_h are the operating cost coefficients of heat-only unit.

(iv) *CHP unit*: as a co-generation unit, it can significantly increase the thermal efficiency and reduce the environment emissions [28] by reusing the heat, thus both the electricity and heat energy can be simultaneously generated, where the total operating cost can be calculated as follows [29]:

$$f_{chp}(P_{chp}, H_{chp}) = \alpha_{chp} + \beta_{chp} P_{chp} + \gamma_{chp} P_{chp}^2 + \delta_{chp} H_{chp} + \theta_{chp} H_{chp}^2 + \xi_{chp} H_{chp} P_{chp} \quad (5)$$

where P_{chp} is the electricity energy output of CHP unit; H_{chp} is the heat energy output of CHP unit; α_{chp} , β_{chp} , γ_{chp} , δ_{chp} , θ_{chp} , and ξ_{chp} are the operating cost coefficients of CHP unit.

(v) *Main grid*: when the microgrid is operated in the grid-connected mode, the main grid can be regarded as an electricity energy supplier if the total electricity energy output of all the DERs is insufficient to balance the total electricity energy demand of all the loads in the microgrid, otherwise it will become an electricity energy demander. Hence, the operating cost from the main grid can be determined by the direction of tie-line power and the current electricity price, as follows:

$$f_{mg}(P_{tie}) = \begin{cases} C_{buy} P_{tie}, & \text{if } P_{tie} \geq 0 \\ C_{sell} P_{tie}, & \text{otherwise} \end{cases} \quad (6)$$

where C_{buy} and C_{sell} are the electricity buying price and selling price, respectively; and P_{tie} is the tie-line power, while a negative P_{tie} will result in a negative operating cost, i.e., the electricity selling profit from the microgrid to the main grid.

2.2. Energy demanders

In order to reduce the peak-valley difference of total power load for an electric power system, the electricity company generally employs a time-of-use pricing strategy to allow the demanders to automatically adjust their electric power consumptions. In general, this process is well known as demand response (DR). Based on the linear demand versus price expression [30], the cost function of each energy demander can be calculated according to the responding power (power curtailment) and his or her sensitiveness of power loads, as follows:

$$f_{\text{dr}}(\Delta D) = \frac{-1}{b^{\text{lin}}} \Delta D^2 + \frac{D_0 - a^{\text{lin}}}{b^{\text{lin}}} \Delta D \quad (7)$$

where ΔD is the responding power; D_0 is the current initial electric power; a^{lin} and b^{lin} are the coefficients of linear demand versus price expression.

2.3. Social welfare and constraints

In this paper, DEM aims to maximize the social welfare (i.e., minimize the total operating cost) of the microgrid while satisfying all the constraints, including energy balance constraint, capacity limits of all energy sources, feasible operating region constraints of CHP units, and minimum demand constraint of each energy demander for the must-run loads. Hence, the mathematical model of DEM of a microgrid can be described as follows [19]:

$$\min f_{\text{cost}} = \sum_{i=1}^{N_{\text{dg}}} f_{\text{dg}}^i(P_{\text{dg}}^i) + \sum_{j=1}^{N_{\text{h}}} f_{\text{h}}^j(H_{\text{h}}^j) + \sum_{k=1}^{N_{\text{chp}}} f_{\text{chp}}^k(P_{\text{chp}}^k, H_{\text{chp}}^k) + \sum_{m=1}^{N_{\text{dr}}} f_{\text{dr}}^m(\Delta D^m) + f_{\text{mg}}(P_{\text{tie}}) \quad (8)$$

subject to

$$\sum_{i=1}^{N_{\text{dg}}} P_{\text{dg}}^i + \sum_{k=1}^{N_{\text{chp}}} P_{\text{chp}}^k + \sum_{l=1}^{N_{\text{wt}}} P_{\text{wt}}^l + \sum_{d=1}^{N_{\text{pv}}} P_{\text{pv}}^d + P_{\text{tie}} - \sum_{m=1}^{N_{\text{dr}}} \Delta D^m = 0 \quad (9)$$

$$\sum_{j=1}^{N_{\text{h}}} H_{\text{h}}^j + \sum_{k=1}^{N_{\text{chp}}} H_{\text{chp}}^k - H_{\text{demand}} = 0 \quad (10)$$

$$P_{\text{dg}}^{i,\min} \leq P_{\text{dg}}^i \leq P_{\text{dg}}^{i,\max}, \quad i = 1, 2, \dots, N_{\text{dg}} \quad (11)$$

$$H_{\text{h}}^{j,\min} \leq H_{\text{h}}^j \leq H_{\text{h}}^{j,\max}, \quad j = 1, 2, \dots, N_{\text{h}} \quad (12)$$

$$P_{\text{chp}}^{k,\min}(H_{\text{chp}}^k) \leq P_{\text{chp}}^k \leq P_{\text{chp}}^{k,\max}(H_{\text{chp}}^k), \quad k = 1, 2, \dots, N_{\text{chp}} \quad (13)$$

$$H_{\text{chp}}^{k,\min}(P_{\text{chp}}^k) \leq H_{\text{chp}}^k \leq H_{\text{chp}}^{k,\max}(P_{\text{chp}}^k), \quad k = 1, 2, \dots, N_{\text{chp}} \quad (14)$$

$$P_{\text{tie}}^{\min} \leq P_{\text{tie}} \leq P_{\text{tie}}^{\max} \quad (15)$$

$$0 \leq \Delta D^m \leq \eta D_0^m, \quad m = 1, 2, \dots, N_{dr} \quad (16)$$

where the superscripts i, j, k, m, l , and d represent the i th DG, the j th heat-only unit, the k th CHP unit, the m th energy demander, the l th WT, and the d th PV unit, respectively; the superscripts min and max represent the lower and upper limits, respectively; N_{dg} is the number of DG; N_h is the number of heat-only units; N_{chp} is the number of CHP units; N_{dr} is the number of energy demanders; N_{wt} is the number of WT; N_{pv} is the number of PV units; and η denotes the maximum allowable power curtailment portion of the current initial electric power, which can ensure the normal operation of must-run loads for the energy demanders.

Note that the operating costs of WT and PV unit are not considered in the total operating cost f_{cost} due to their inherent zero fuel consumption. Moreover, the feasible operating region constraints of CHP units (13) and (14) indicate that the electricity energy output and heat energy output are tightly coupled, as clearly illustrated in Fig. 1. It can be observed that the energy outputs of CHP units should be enclosed by the boundary curve ABCDEF (i.e., the feasible operating region) [23], where both the lower and upper limits of electricity energy output are determined by different heat energy outputs and vice versa. In order to reduce the optimization difficulty, DEM of a microgrid is decomposed into two optimization subtasks. The first one is responsible for optimizing the tie-line power and the heat energy outputs of CHP units, which is relatively complex with a nondifferentiable operating cost from the main grid (6) and the feasible operating region constraints. Based on the decision results of the first optimization subtasks, the second one with the rest of operating cost and constraints is essentially a convex optimization and relatively easy to be addressed.

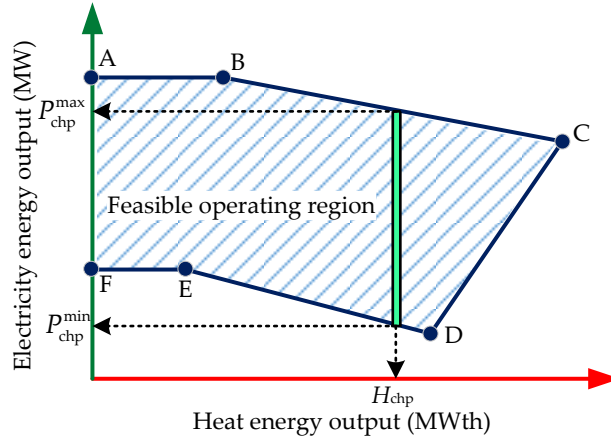


Fig. 1 Feasible operating region of CHP units.

3. CPSS with parallel learning for DEM

3.1. CPSS framework for DEM of a microgrid

As illustrated in Fig. 2, CPSS is a complex system with three dimensions, including physical space, cyberspace, and social space, and all of them are tightly connected via the cyberspace [6]. For DEM of a microgrid, the main task of CPSS is to

maximize the social welfare and to react to the physical space. Compared with CPS, the major improvement part of CPSS is the social space with human beings, such as human behaviors and human interactions. For each optimization task, each energy supplier or energy demander firstly acquires the current operating parameters of the corresponding distributed device from the physical space, then each of them will autonomously make a dispatch decision through the interaction with others in social space based on the communication and computation in cyberspace with parallel learning, finally the optimal dispatch strategy will be issued to each distributed device for optimal control in the physical space.

For effectively searching a high quality dispatch strategy, a CE based general-sum game with model-free Q-learning [24] is used for achieving the human interaction on the complex optimization subtask, while the novel adaptive consensus algorithm is implemented for human interaction on the simple optimization subtask.

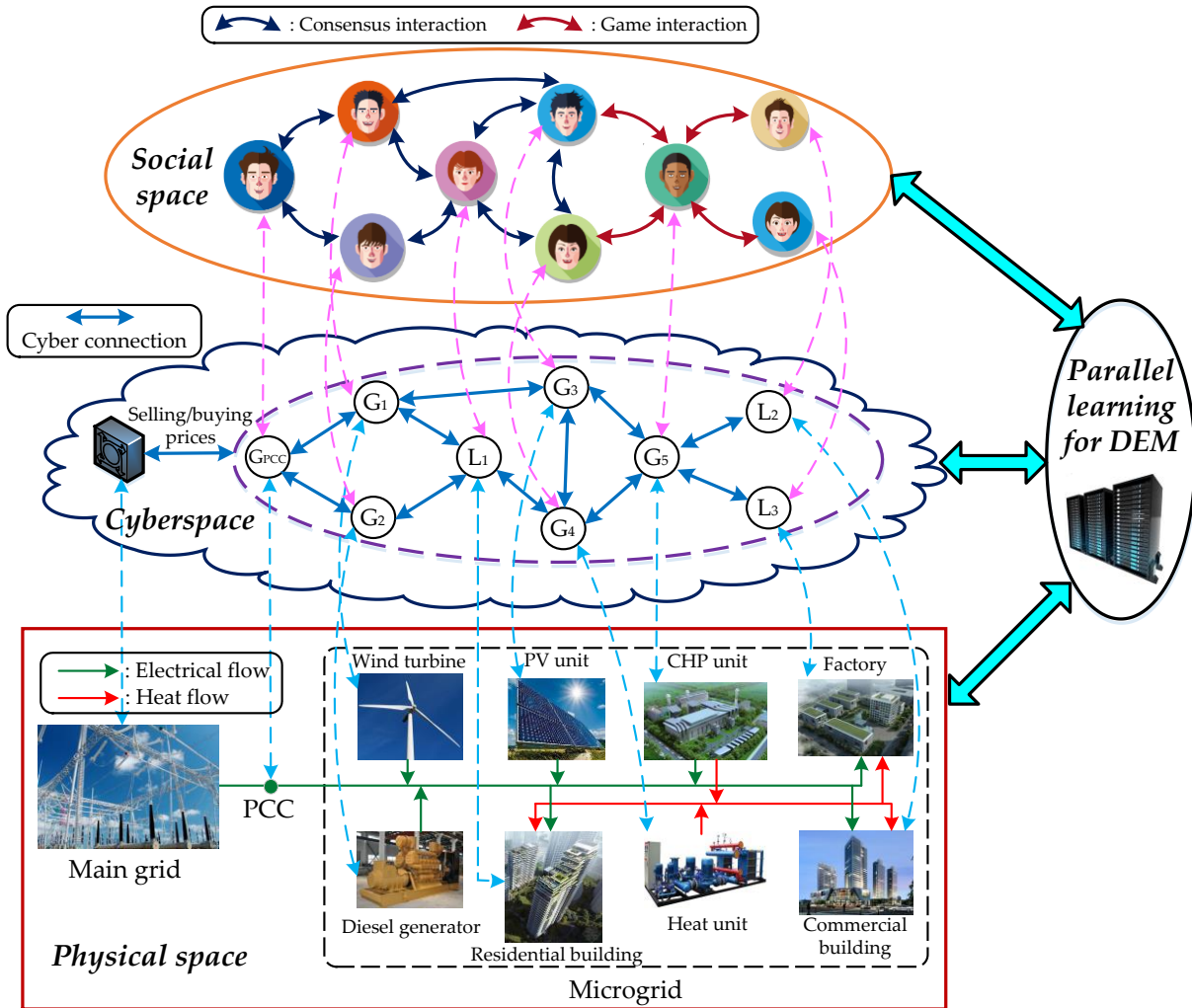


Fig. 2 CPSS framework for DEM of a microgrid.

3.2. Parallel learning with multiple parallel systems

According to the real-world system, multiple parallel VASs [31] are constructed for different evolutions of DEM in a microgrid. In this paper, the real-world system mainly provide the optimization model (8)-(16), the current best solution, and the

183 energy management knowledge of each agent to multiple VASs, then each VAS can generate an optimal dispatch strategy via
 184 the human interactions and risk-free trial-and-error, while the energy management knowledge of each agent will be updated.
 185 Consequently, the parallel n -VASs will vote for n optimal dispatch strategies and provide their energy management knowledge
 186 to the real-world system, while each VAS will improve its dispatch strategy and energy management knowledge through
 187 learning from its interactive VASs based on small world network, as shown in Fig. 3.

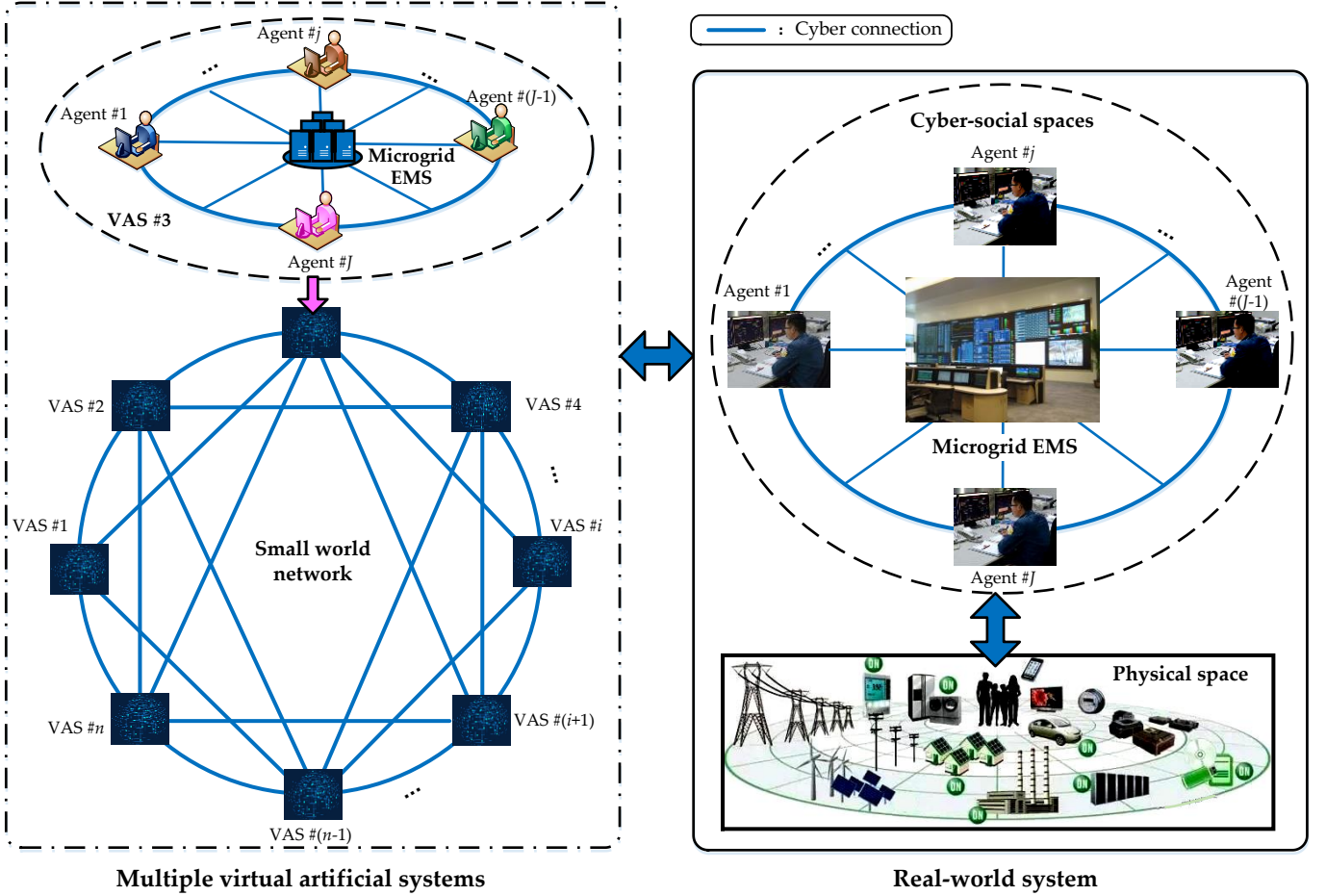


Fig. 3 Parallel learning with multiple virtual artificial systems and a real-world system.

3.2.1 CE based human interaction on complex optimization subtask

(i) CE based general-sum game

For a general-sum game, a CE is more general than a Nash equilibrium as the set of Nash equilibria is wholly included in the set of correlated equilibria [24]. Generally speaking, a CE is a probability distribution of joint actions from which no agent is motivated to deviate unilaterally, which can be combined with Q-learning, as follows:

$$\left\{ \begin{array}{l} \sum_{\vec{a}_{-j} \in A_{-j}(s_k)} \pi_j(s_k, \vec{a}) Q_j^k(s_k, (\vec{a}_{-j}, a_j)) \geq \sum_{\vec{a}_{-j} \in A_{-j}(s_k)} \pi_j(s_k, \vec{a}) Q_j^k(s_k, (\vec{a}_{-j}, a_j^o)) \\ A_{-j} = \prod_{p \neq j} A_p, \vec{a}_{-j} = \prod_{p \neq j} a_p, \vec{a} = (\vec{a}_{-j}, a_j), a_j^o \neq a_j \end{array} \right. \quad (17)$$

where π_j is the probability distributions of state-action pairs of the j th agent, which can be called a CE when it satisfies the

inequality constraint (17); \mathbf{Q}_j^k is the knowledge matrix of the j th agent at the k th iteration, which represent the knowledge values of station action pairs; s_k is the state of the multi-agent system at the k th iteration; $\vec{a}=[a_1, \dots, a_j, \dots, a_J]$ is the joint action of all the agents; a_j is the action of the j th agent; J is the number of agents; \vec{a}_{-j} is the joint action of all the agents except the j th agent; $\mathbf{A}(s_k)$ is the agents' set of available joint actions in state s_k ; \mathbf{A}_j is the j th agent's set of pure actions; and a_j^o is the j th agent's any other action except a_j .

(ii) Knowledge learning

According to the state-action-reward-state data via continuous interactions with the environment, each agent can update its own knowledge of different state-action pairs with the feedback rewards by reinforcement learning. In this paper, Q-learning is used for achieving this learning process, thus the knowledge can be stored by the Q-value matrix, as follows [32]:

$$V_j(s_{k+1}) = \sum_{\vec{a} \in \mathbf{A}(s_{k+1})} \pi_j(s_{k+1}, \vec{a}) \mathbf{Q}_j^k(s_{k+1}, \vec{a}) \quad (18)$$

$$\mathbf{Q}_j^{k+1}(s_k, \vec{a}) = \mathbf{Q}_j^k(s_k, \vec{a}) + \alpha \left[(1-\gamma) R_j(s_k, \vec{a}) + \gamma V_j(s_{k+1}) - \mathbf{Q}_j^k(s_k, \vec{a}) \right] \quad (19)$$

where $V_j(s_{k+1})$ denotes the state value-function of the j th agent for state s_{k+1} ; α is the knowledge learning factor; γ is the discount factor; and $R_j(s_k, \vec{a})$ is the feedback reward after implementing a joint action \vec{a} at the state s_k .

(iii) Decision strategies

In the complex optimization subtask, the strategy decision of each agent is divided into two processes. Firstly, each agent choose a pure action strategy (i.e., interval of optimization) according to its preference behavior, then an accurate solution can be determined by the non-uniform mutation operator based on the local optimum of the corresponding interval. In this paper, four human decision strategies are introduced to each agent for selecting a pure action, as [24]

- *Utilitarian behavior*: maximize the sum of all agents' benefits, as follows:

$$\max f_b(\pi_j) = \sum_{j=1,2,\dots,J} \sum_{\vec{a} \in \mathbf{A}(s_k)} \pi_j(s_k, \vec{a}) \mathbf{Q}_j^k(s_k, \vec{a}) \quad (20)$$

- *Egalitarian behavior*: maximize the minimum of all agents' benefits, as follows:

$$\max f_b(\pi_j) = \min_{j=1,2,\dots,J} \sum_{\vec{a} \in \mathbf{A}(s_k)} \pi_j(s_k, \vec{a}) \mathbf{Q}_j^k(s_k, \vec{a}) \quad (21)$$

- *Plutocratic behavior*: maximize the maximum of all agents' benefits, as follows:

$$\max f_b(\pi_j) = \max_{j=1,2,\dots,J} \sum_{\vec{a} \in \mathbf{A}(s_k)} \pi_j(s_k, \vec{a}) \mathbf{Q}_j^k(s_k, \vec{a}) \quad (22)$$

- *Dictatorial behavior*: maximize the maximum of any individual agent's benefits, as follows:

$$\max f_b(\pi_j) = \sum_{\vec{a} \in \mathbf{A}(s_k)} \pi_j(s_k, \vec{a}) \mathbf{Q}_j^k(s_k, \vec{a}) \quad (23)$$

where f_b is the behavior function, in which the maximum and the corresponding optimal CE can be calculated by linear

programming with the inequality constraints (17) and the following constraints, as

$$\sum_{\vec{a} \in A(s_k)} \pi_j(s_k, \vec{a}) = 1, \quad 0 \leq \pi_j(s_k, \vec{a}) \leq 1 \quad (24)$$

After acquiring the optimal CE π_j^* , a pure action of each agent and an accurate dispatch strategy can be determined. Aiming at a proper trade-off between exploration and exploitation, the ε -Greedy rule [33] is used for interval selection, as

$$a_j = \begin{cases} \arg \max_{a_j \in A_j} \pi_j(s_k, (a_{-j}, a_j)), & \text{if } q_0 \leq \varepsilon \\ a_{\text{rand}}, & \text{otherwise} \end{cases} \quad (25)$$

$$x_j^k = \begin{cases} x_j^{\text{best}}(a_j) + \Delta[k, x_j^{\text{ub}}(a_j) - x_j^{\text{best}}(a_j)], & \text{if } \text{rand}(0,1) < 0.5 \\ x_j^{\text{best}}(a_j) - \Delta[k, x_j^{\text{best}}(a_j) - x_j^{\text{lb}}(a_j)], & \text{otherwise} \end{cases} \quad (26)$$

$$\begin{cases} x_j^{\text{ub}}(a_j) = x_j^{\min} + a_j \cdot (x_j^{\max} - x_j^{\min}) / |A_j| \\ x_j^{\text{lb}}(a_j) = x_j^{\min} + (a_j - 1) \cdot (x_j^{\max} - x_j^{\min}) / |A_j| \end{cases} \quad (27)$$

$$\Delta[k, y] = y \cdot \left(1 - r^{(1-k/k_{\max})^b}\right) \quad (28)$$

where q_0 is a uniform random value from $[0, 1]$; ε is the exploitation rate which represents the probability of exploitation; a_{rand} denotes a random action (exploration) chosen from the action space A_j ; $x_j^{\text{best}}(a_j)$ is the previous best optimal solution at the action (a_j) interval of the j th controllable variable; $x_j^{\text{ub}}(a_j)$ and $x_j^{\text{lb}}(a_j)$ are the upper and lower bounds of the action (a_j) interval, respectively; x_j^{\min} and x_j^{\max} are the minimum and maximum values of the j th controllable variable, respectively; $\Delta[k, y]$ is a decay function as the iteration k increases; r is a uniform random value from $[0, 1]$; b is the system parameter which determines the degree of non-uniformity; and k_{\max} is the maximal iteration number.

3.2.2 Adaptive consensus algorithm based human interaction on simple optimization subtask

(i) Graph theory of interaction network

The interaction network among humans can be typically built with a directed graph $G=(V, E, A)$, where $V=\{v_1, v_2, \dots, v_N\}$ is the set of nodes (agents); $E \subseteq V \times V$ denotes the edges (interactions); and $A=[a_{pq}] \in R^{N \times N}$ is a weighted adjacency matrix [34]. Based on these most basic elements, the Laplacian matrix $L=[l_{pq}] \in R^{N \times N}$ and row stochastic matrix $D=[d_{pq}] \in R^{N \times N}$ of the graph G can be calculated as follows:

$$l_{pp} = \sum_{p=1, q \neq p}^N a_{pq}, l_{pq} = -a_{pq}, \forall p \neq q \quad (29)$$

$$d_{pq}[k] = |l_{pq}| / \sum_{q=1}^N |l_{pq}|, \quad p = 1, 2, \dots, N \quad (30)$$

(ii) Adaptive consensus algorithm on incremental cost

The adaptive consensus algorithm inherently represents a herd behavior of human interactions, i.e., each agent will regulate

its own state to reach a consensus with the adjacent agents after acquiring their current states. In this paper, the first-order adaptive consensus algorithm is adopted for this consensus process, as follows [35]:

$$s_p[k+1] = \sum_{q=1}^N d_{pq}[k] s_q[k] \quad (31)$$

where s_p is the state of the p th agent.

Note that the simple optimization subtask only has a unique minimum point as it is a strictly convex optimization, thus its global optimum can be obtained when all the agents can reach a consensus on the incremental cost while satisfying various constraints. Hence, the incremental cost is taken as the consensus state for human interactions, which can be written as [14]

$$\lambda_p = \frac{\partial f_p(x_p)}{\partial x_p} = \kappa_p x_p + \varphi_p \quad (32)$$

where λ_p is the incremental cost of the p th agent; x_p is the controllable variable (energy output or demand) of the p th agent; κ_p and φ_p are the incremental cost coefficients of the p th agent, respectively, which can be determined by the corresponding cost coefficients; and f_p is the operating cost of the p th agent.

In order to satisfy the energy balance constraints (9)-(10), the electricity energy mismatch ΔE and heat energy mismatch ΔH between the energy suppliers and energy demanders are introduced in adaptive consensus algorithm, as follows:

$$\Delta E = \sum_{i=1}^{N_{dg}} P_{dg}^i + \sum_{k=1}^{N_{chp}} P_{chp}^k + \sum_{l=1}^{N_{wt}} P_{wt}^l + \sum_{d=1}^{N_{pv}} P_{pv}^d + P_{tie} - \sum_{m=1}^{N_{dr}} \Delta D^m \quad (33)$$

$$\Delta H = \sum_{j=1}^{N_h} H_h^j + \sum_{k=1}^{N_{chp}} H_{chp}^k - H_{demand} \quad (34)$$

It can be found from (32) that an increasing incremental cost will lead to an increasing energy output and an decreasing energy demand, thus the consensus interaction should be carefully designed to satisfy the energy balance constraints following this changing rule, as follows:

- *Unified consensus*: if the signs of ΔE and ΔH are consistent, i.e., $\Delta E \cdot \Delta H \geq 0$, then all the agents can update their incremental cost state in an unified interaction network, as

$$\lambda_p[k+1] = \begin{cases} \sum_{q=1}^N d_{pq}[k] \lambda_q[k] - \mu \Delta E, & p \in \Omega_E \\ \sum_{q=1}^N d_{pq}[k] \lambda_q[k] - \mu \Delta H, & p \in \Omega_H \end{cases} \quad (35)$$

- *Independent consensus*: if the signs of ΔE and ΔH are inconsistent, i.e., $\Delta E \cdot \Delta H < 0$, then the electricity agents and heat agents need to be separated to update their incremental cost state in two independent interaction network, as

$$\lambda_p[k+1] = \begin{cases} \sum_{q \in \Omega_E} d_{pq}^E[k] \lambda_q[k] - \mu \Delta E, & p \in \Omega_E \\ \sum_{q \in \Omega_H} d_{pq}^H[k] \lambda_q[k] - \mu \Delta H, & p \in \Omega_H \end{cases} \quad (36)$$

where Ω_E and Ω_H represent the sets of electricity agents and heat agents, respectively; d_{pq}^E is the (p,q) entry of the row stochastic matrix of the interaction network among the electricity agents; d_{pq}^H is the (p,q) entry of the row stochastic matrix of the interaction network among the heat agents; and μ denotes the adjustment factor of energy mismatch, $\mu > 0$.

Therefore, each agent will regulate its incremental cost between these two consensus mode according to the sign of $(\Delta E \cdot \Delta H)$, as illustrated in Fig. 4.

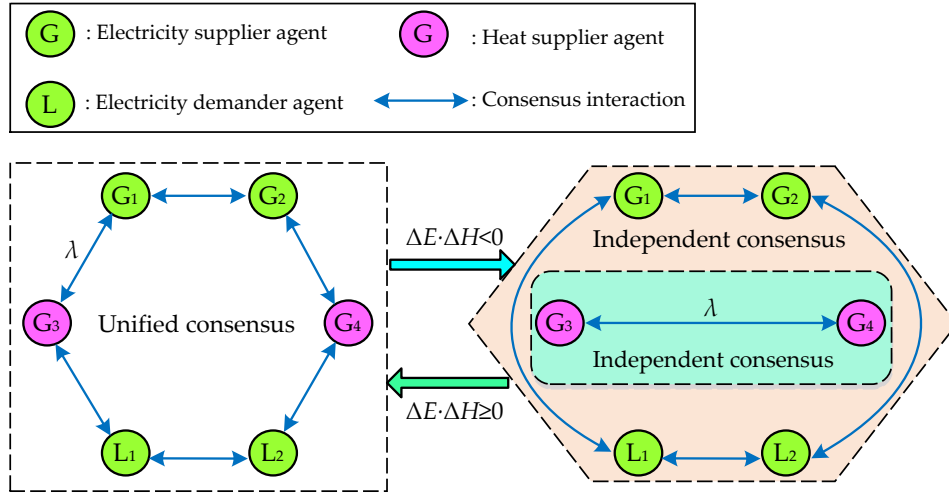


Fig. 4 Principle of human interaction by adaptive consensus algorithm.

By fully considering the lower and upper limits of each controllable variable (11)-(16), the energy output or demand of each agent can be determined based on (32), as follows [14]:

$$x_p^c = \frac{\lambda_p[k] - \varphi_p}{\kappa_p} \quad (37)$$

$$x_p^k = \begin{cases} x_p^{\min}, & \text{if } x_p^c < x_p^{\min} \\ x_p^c, & \text{if } x_p^{\min} \leq x_p^c \leq x_p^{\max} \\ x_p^{\max}, & \text{if } x_p^c > x_p^{\max} \end{cases} \quad (38)$$

where x_p^c denotes the energy consensus value of the p th agent; x_p^{\min} and x_p^{\max} are the minimum and maximum values of the p th controllable variable, respectively.

3.2.3 Interaction between different parallel systems

(i) Interaction between VASs and the real-world system

In the initial phase, the real-world system will provide the prior energy management knowledge \mathbf{Q}^{p*} ($j=1,2,\dots, J$) and the optimal incremental cost λ^* of a similar optimization task to each VAS, which can be regarded as the initial knowledge matrices

289 \mathbf{Q}_j^{i0} and the initial incremental cost λ of each agent. On the other hand, the agent of real-world system will update its current best
 290 solution and the knowledge matrix according to the current solutions of VASs, as follows:

$$291 \quad h = \arg \min_{i=1,2,\dots,n} f_{\text{cost}}(\mathbf{x}^{ik}) \quad (39)$$

$$292 \quad \mathbf{x}_b^{rk} = \begin{cases} \mathbf{x}^{hk}, & \text{if } f_{\text{cost}}(\mathbf{x}_b^{rk}) \geq f_{\text{cost}}(\mathbf{x}^{hk}) \\ \mathbf{x}_b^{rk}, & \text{otherwise} \end{cases} \quad (40)$$

$$293 \quad \mathbf{Q}_j^{rk} = \begin{cases} \mathbf{Q}_j^{rk} + r_Q \cdot (\mathbf{Q}_j^{hk} - \mathbf{Q}_j^{rk}), & \text{if } f_{\text{cost}}(\mathbf{x}_b^{rk}) \geq f_{\text{cost}}(\mathbf{x}^{hk}) \\ \mathbf{Q}_j^{rk}, & \text{otherwise} \end{cases} \quad (41)$$

294 where \mathbf{x}^{ik} represent the current solution of the i th VAS, which consists of all the controllable variables; h denotes the current best
 295 VAS with the smallest total operating cost; \mathbf{x}_b^{rk} is the current best solution of the real-world system; r_Q is the random matrix
 296 from [0,1] with the same scale of knowledge matrix; and \mathbf{Q}_j^{rk} is the current knowledge matrix of the j th agent in the real-world
 297 system.

298 (ii) Interaction among VASs

299 Generally speaking, the larger otherness between different VASs will lead to more diverse dispatch strategies, which can
 300 effectively avoid the low-quality local optimum, but it will consume more computation time to search the potential global
 301 optimum. To properly balance them, the small world network is used for constructing the interaction network among VASs, in
 302 which each VAS can stochastically interact with any other VASs with a decreasing probability, as follows [36]:

$$303 \quad \rho_{iw} = \left(1 - \frac{k}{k_{\max}}\right) \cdot C_p, \quad w = 1, 2, \dots, n \quad (42)$$

304 where ρ_{iw} is the interaction probability between the i th VAS and the w th VAR; k_{\max} is the maximal iteration number; and C_p is the
 305 probability coefficient, with $0 < C_p < 1$.

306 Similarly, each VAS will update its current best solution and the knowledge matrix according to the current solutions of its
 307 interactive VASs, as follows:

$$308 \quad h^i = \arg \min_{w \in \Omega_i} f_{\text{cost}}(\mathbf{x}^{wk}) \quad (43)$$

$$309 \quad \mathbf{x}_b^{ik} = \begin{cases} \mathbf{x}^{h^i k}, & \text{if } f_{\text{cost}}(\mathbf{x}_b^{ik}) \geq f_{\text{cost}}(\mathbf{x}^{h^i k}) \\ \mathbf{x}_b^{ik}, & \text{otherwise} \end{cases} \quad (44)$$

$$310 \quad \mathbf{Q}_j^{ik} = \begin{cases} \mathbf{Q}_j^{ik} + r_Q \cdot (\mathbf{Q}_j^{h^i k} - \mathbf{Q}_j^{ik}), & \text{if } f_{\text{cost}}(\mathbf{x}_b^{ik}) \geq f_{\text{cost}}(\mathbf{x}^{h^i k}) \\ \mathbf{Q}_j^{ik}, & \text{otherwise} \end{cases} \quad (45)$$

311 where h^i denotes the current best VAS in the i th VAR's interactive network; Ω_i is the VAR set in the i th VAS's interactive
 312 network, which can be determined by (42); \mathbf{x}_b^{ik} is the current best solution of the i th VAS; and \mathbf{Q}_j^{ik} is the current knowledge

matrix of the j th agent in the i th VAS.

3.3 Application design for DEM

3.3.1 Communication information in each learning system

As shown in Fig. 3, all the agents will communicate with the microgrid energy management system (EMS), in which each agent will transmit its current optimal energy output or demand to the microgrid EMS. For the complex optimization subtask, the microgrid EMS is regarded as an external environment for each learning agent, thus each agent can acquire the state and feedback reward after implementing an optimal CE action. Besides, each learning agent can access the current actions and knowledge matrices of other agents at any time. For the simple optimization subtask, the microgrid EMS will continuously issue the energy mismatches to each agent, thus the consensus collaboration among the agents can be achieved.

3.3.2 Design of feedback reward

To maximize the social welfare, the feedback reward should be designed to match the total operating cost f_{cost} in (8), i.e., a smaller f_{cost} encourages a larger feedback reward, which can be calculated as follows:

$$R_j(s_k, \vec{a}) = C_1 - \left(f_j(x_j^k) + \frac{1}{J} \sum_{p=1, p \neq j}^N f_p(x_p^k) \right) / C_2 \quad j=1, 2, \dots, J \quad (46)$$

where f_j is the operating cost of the j th learning agent; C_1 and C_2 are the feedback reward coefficients.

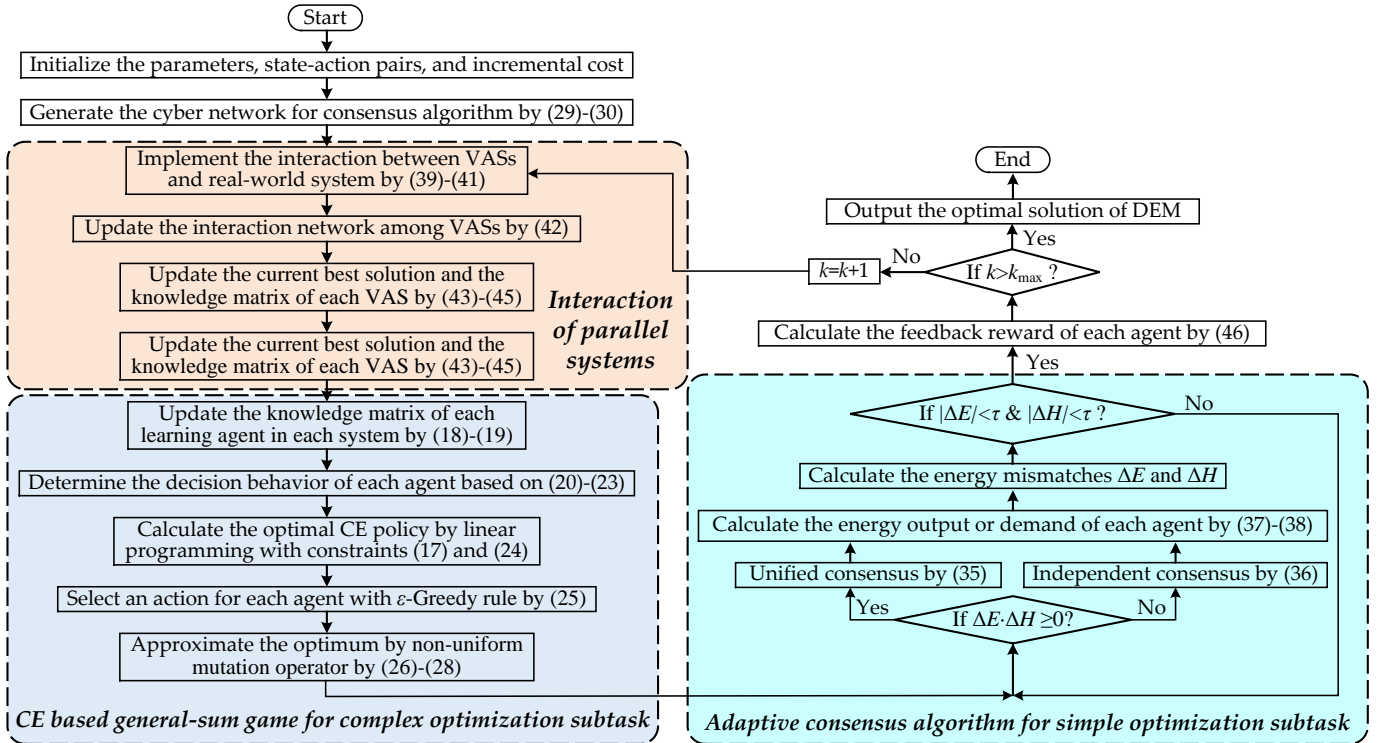


Fig. 5 Execution procedure of CPSS with parallel learning for DEM of a microgrid.

3.3.3 Execution procedure

In summary, the CPSS with parallel learning for DEM of a microgrid is given in Fig. 5, where τ is the energy mismatch tolerance, which is set to be 0.0001 in this paper. Note that each agent will prefer to produce a decision behavior from (20)-(23) based on a probability distribution, which is set to be [0.7, 0.1, 0.1, 0.1] for utilitarian, egalitarian, plutocratic, and dictatorial, respectively.

4. Case studies

4.1 Simulation model

The testing microgrid [19] is operated in grid-connected mode, which contains 11 energy suppliers, 7 energy demanders, where the complex optimization subtask is composed of tie-line power and the heat energy outputs of CHP units, while the simple optimization subtask consists of the rest controllable variables, as shown in Fig. 6. The main parameters of testing microgrid are given in Appendix. Furthermore, the switching cyber connection is designed around the heat unit (Heat₁), i.e., if $\Delta E \cdot \Delta H \geq 0$, then Heat₁ will simultaneously connect with L₁, L₂, and DG₁, otherwise, Heat₁ will disconnect with them, while L₁ and L₂ will connect with each other. To construct the human participations in real-world system, thirteen experimenters are employed as the controllers for each energy supplier or demander, respectively. Through trial-and-error, the main parameters of parallel learning are given in Table 1.

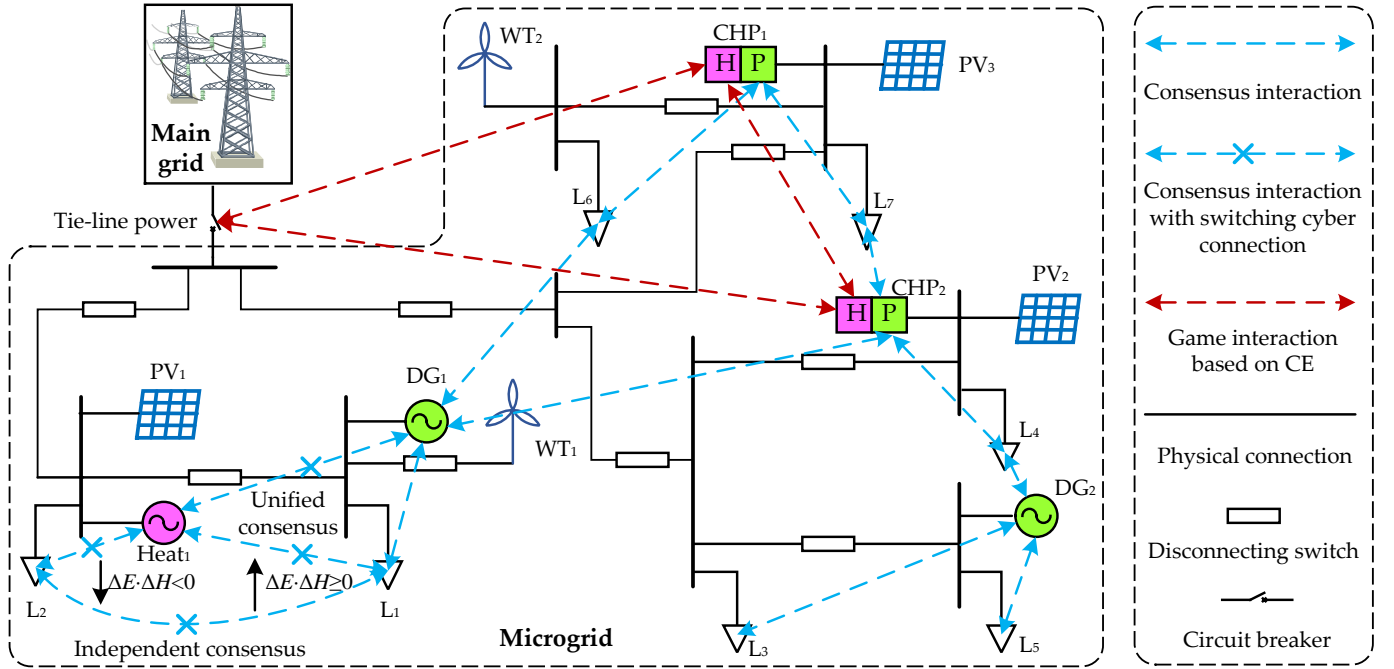


Fig. 6 CPSS of the testing microgrid.

In order to verify the performance of the proposed technique, four commonly used heuristic algorithms are introduced for comparisons, including genetic algorithm (GA) [37], particle swarm optimization (PSO) [38], artificial bee colony (ABC) [39], group search optimizer (GSO) [40], where population size and maximum iteration number are set to be 50 and 250, respectively.

Moreover, all the simulations are undertaken in Matlab R2016a by a small server with Intel(R) Xeon (R) E5-2670 v3 CPU at 2.3 GHz with 64 GB of RAM.

Table 3

The main parameters of parallel learning.

Parameter	Range	Value
α	$0 < \alpha < 1$	0.9
γ	$0 < \gamma < 1$	0.1
ε	$0 < \varepsilon < 1$	0.9
μ	$\mu > 0$	3
C_p	$0 < C_p < 1$	0.9
C_1	$C_1 > 0$	1
C_2	$C_2 > 0$	1000
k_{\max}	$k_{\max} > 0$	250

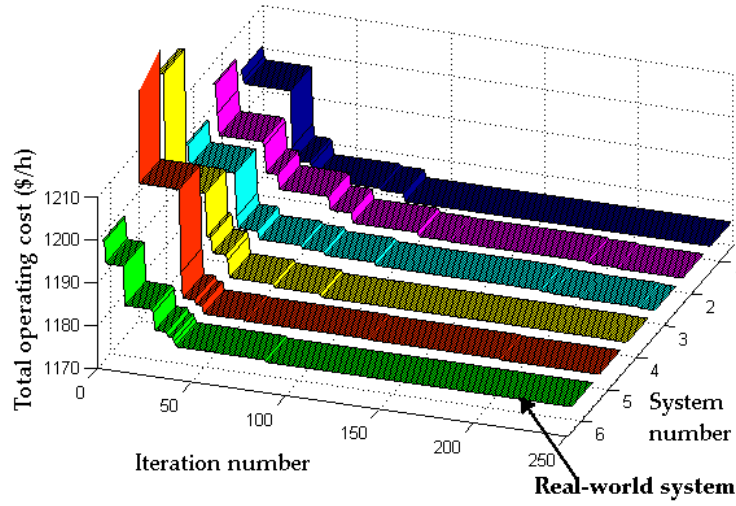


Fig. 7 Convergence of parallel learning in different systems.

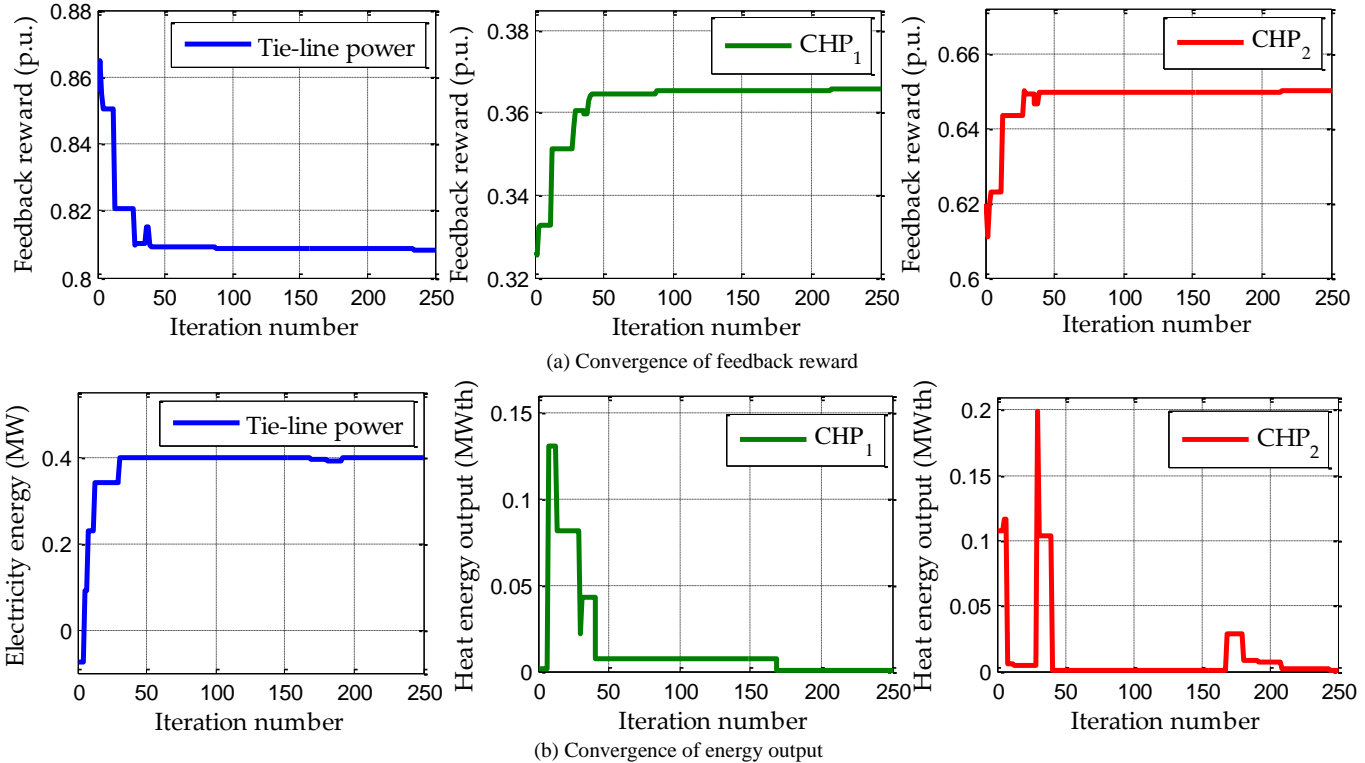


Fig. 8 Convergence of CE based human interaction in the real-world system.

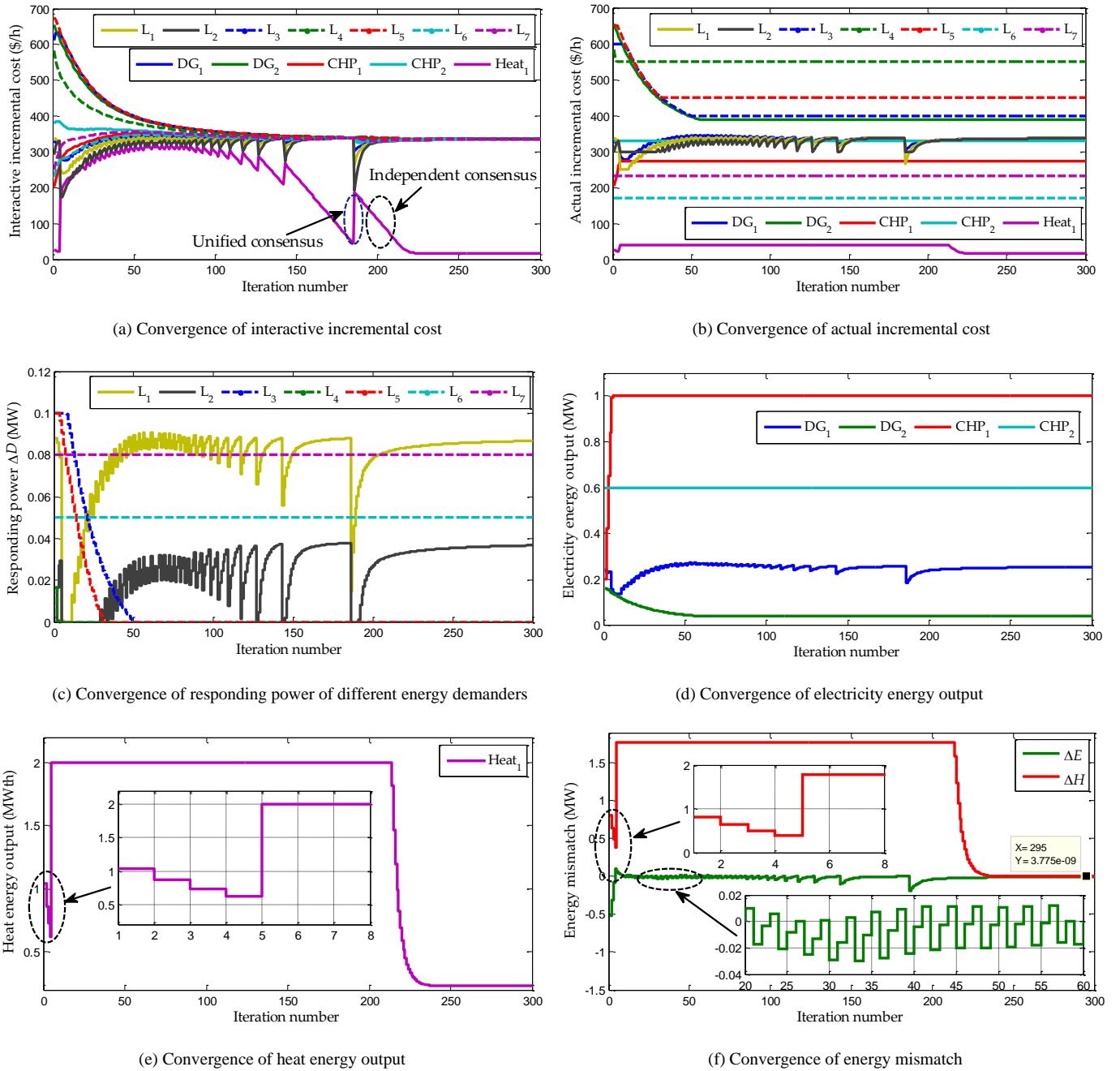


Fig. 9 Convergence of adaptive consensus algorithm based human interaction in the real-world system at the final game iteration.

4.2 Study of convergence

Figs. 7-9 provide the convergence of parallel learning under scenario 3 (at 14:00) with peak price, where the number of VASs is set to be 5. It can be found from Fig. 7 that each system can converge to a high-quality optimal solution with a lower total operating cost via an effective interaction with other systems, especially for the real-world system. At the same time, three energy suppliers (tie-line power, CHP_1 , and CHP_2) can achieve an optimal CE among them after around 200 CE based game iterations, while the feedback reward of each one will increase as its energy output decrease and vice versa, as illustrated in Fig. 8. After each game iteration, twelve energy agents (suppliers and demanders) will interact their incremental costs for reaching a

consensus by adaptive consensus algorithm. As shown in Fig. 9(a), the interactive incremental cost will update between unified consensus mode and independent consensus mode according to the dynamic energy mismatches, in which the heat-only unit Heat₁ cannot reach a consensus with other electricity energy agents due to the heat energy balance constraint (10). Besides, the actual incremental costs of some energy agents have reached their limits after a fewer interactions, thus their energy outputs or responding power can strictly satisfy their capacity lower and upper limits, as shown in Fig. 9(b)-(e). Finally, both the electricity and heat energy mismatches (ΔE and ΔH) simultaneously satisfy the energy mismatch tolerance after a series of corrections (See Fig. 9(f)), i.e., $|\Delta E| < \tau$ and $|\Delta H| < \tau$.

Table 4

Comparative results of optimal solutions obtained by different algorithms under scenario 3.

Demanders or Suppliers	Energy type	Optimal energy generations and consumptions (MW)				
		GA	PSO	ABC	GSO	Parallel learning
L ₁	Electricity	0.419	0.410	0.422	0.432	0.412
	Heat	0.030	0.030	0.030	0.030	0.030
L ₂	Electricity	0.371	0.357	0.344	0.385	0.362
	Heat	0.030	0.030	0.030	0.030	0.030
L ₃	Electricity	0.597	0.600	0.581	0.600	0.600
	Heat	0.040	0.040	0.040	0.040	0.040
L ₄	Electricity	0.448	0.450	0.409	0.450	0.450
	Heat	0.030	0.030	0.030	0.030	0.030
L ₅	Electricity	0.540	0.550	0.542	0.550	0.550
	Heat	0.040	0.040	0.040	0.040	0.040
L ₆	Electricity	0.451	0.450	0.461	0.454	0.450
	Heat	0.040	0.040	0.040	0.040	0.040
L ₇	Electricity	0.279	0.270	0.282	0.270	0.270
	Heat	0.020	0.020	0.020	0.020	0.020
PV ₁	Electricity	0.100	0.100	0.100	0.100	0.100
PV ₂	Electricity	0.100	0.100	0.100	0.100	0.100
PV ₃	Electricity	0.100	0.100	0.100	0.100	0.100
WT ₁	Electricity	0.200	0.200	0.200	0.200	0.200
WT ₂	Electricity	0.300	0.300	0.300	0.300	0.300
Tie-line power	Electricity	0.355	0.399	0.387	0.399	0.399
DG ₁	Electricity	0.325	0.248	0.261	0.308	0.255
DG ₂	Electricity	0.040	0.040	0.096	0.041	0.040
CHP ₁	Electricity	0.993	1.000	0.923	0.999	1.000
	Heat	0.009	0.000	0.047	0.001	0.000
CHP ₂	Electricity	0.591	0.600	0.573	0.594	0.599
	Heat	0.026	0.000	0.152	0.015	0.000
Heat ₁	Heat	0.195	0.230	0.031	0.215	0.226
Total operating cost f_{cost} (\$/h)		1182.886	1176.073	1210.318	1178.385	1176.021

4.3 Comparative results and discussions

Fig. 10 shows the convergence of total operating costs obtained by different algorithms under scenario 3. It is clear that both parallel learning and PSO outperform other three algorithms because each of them can obtain a lower total operating cost in a fewer iterations. Moreover, the detailed optimal dispatch strategies of all the energy suppliers and demanders obtained by different algorithms are listed in Table 3. It verifies that the proposed parallel learning can not only realize the distributed optimization of DEM with human participation and interaction, but also can guarantee the quality of the obtained optimal solution compared with the commonly used centralized heuristic algorithms, which results from the deep exploitations and

explorations with various decision strategies (20)-(23) in multiple VASs.

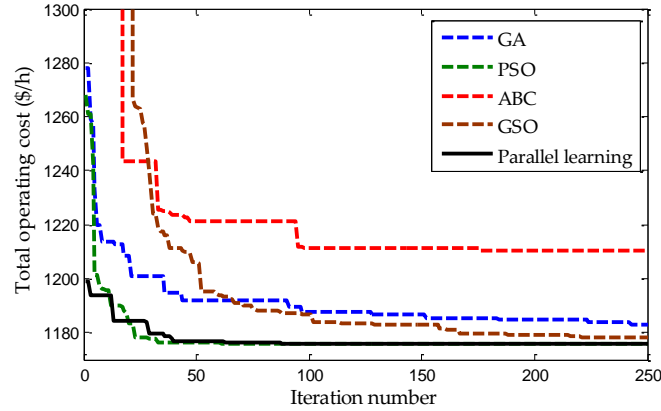
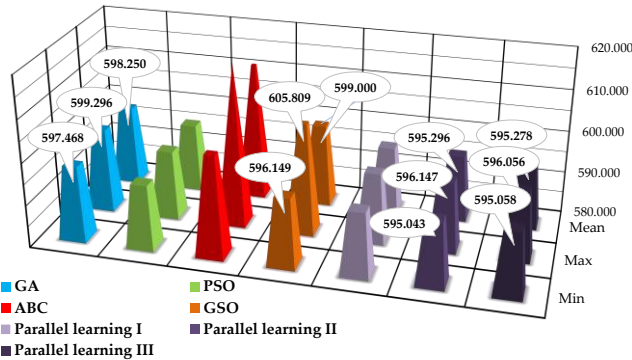
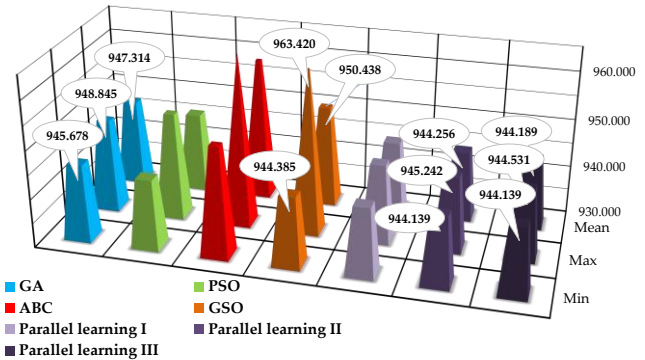


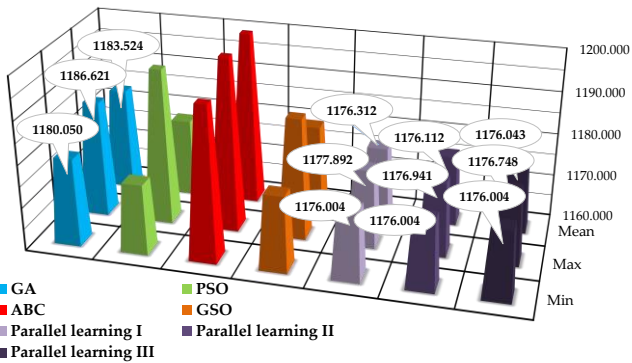
Fig. 10 Convergence of total operating costs obtained by different algorithms under scenario 3.



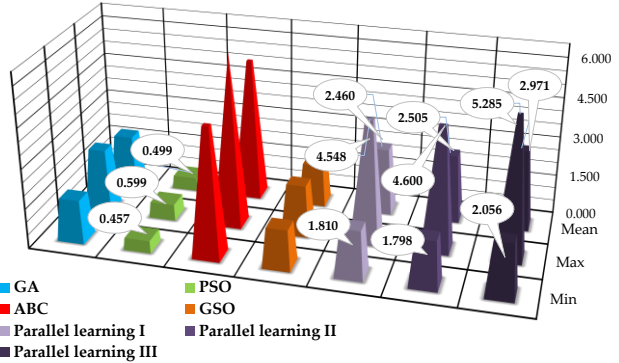
(a) Obtained total operating costs under scenario 1



(b) Obtained total operating costs under scenario 2



(c) Obtained total operating costs under scenario 3



(d) Execution time of each scenario

Fig. 11 Statistical results obtained by different algorithms under three scenarios in 50 runs.

In order to further test the performance of parallel learning, all the algorithms are implemented for three different scenarios (See Table A.5) with 50 independent runs. Fig. 11 shows the statistical results obtained by them, where parallel learning I, parallel learning II, and parallel learning III represent the parallel learning with different numbers of VASs, i.e., 5, 10, and 15 respectively. It also proves that parallel learning can search the highest quality optimal solution with a lowest total operating cost under each scenario, especially parallel learning with more VASs. This obviously demonstrates that the increasing VASs can generate a potential higher quality optimal solution via a deeper exploitation and exploration with various decision strategies.

However, it requires more computation capability and consumes more execution time, as shown in Fig. 11(d). Furthermore, the execution time of parallel learning is slightly larger than that of GA, PSO, and GSO since each game agent requires a linear programming computation to search an optimal CE policy at each iteration.

6. CONCLUSION

In this paper, a novel CPSS with parallel learning has been proposed for DEM of a microgrid. The main contributions can be summarized as follows

(i) The proposed CPSS is constructed by considering the human participation and interaction in social space, which can widely yield potential optimal distributed strategies for DEM in a real-world microgrid.

(ii) The CE based human interaction with various decision strategies can efficiently search an optimal dispatch strategy of a complex optimization subtask of DEM, including the tie-line power with a nondifferentiable objective function, and the CHP units with complex feasible operating regions constraints.

(iii) The adaptive consensus algorithm based human interaction can effectively achieve the self-organization of each human with local communications, while the switch between unified consensus and independent consensus can simultaneously satisfy the consensus requirement and the multi-energy balance constraints.

(iv) The real-world system can continuously learn the knowledge from multiple virtual VASs, in which a deep exploitation and exploration can be implemented in each VAS. Hence, the quality of the obtained optimal solution of DEM can be guaranteed for the real-world system without any adverse trials, i.e., a lower total operating cost (higher social welfare) of a microgrid can be obtained.

Acknowledgment

The authors gratefully acknowledge the support of National Natural Science Foundation of China (51477055, 51777078).

Appendix

Table A.1

Parameters of DGs and heat-only units.

Units	Operating cost coefficients			Capacity (MW)	
	α_i	β_i	γ_i	Minimum	Maximum
DG ₁	10.193	210.36	250.2	0	0.5
DG ₂	2.305	301.4	1100	0.04	0.2
Heat ₁	33	12.3	6.9	0	2

Table A.2

Operating cost coefficients of CHP units.

Units	α_i	β_i	γ_i	δ_i	θ_i	ζ_i
CHP ₁	339.5	185.7	44.2	53.8	38.4	40
CHP ₂	100	288	34.5	21.6	21.6	8.8

Table A.3

Electricity buying and selling prices from the main grid.

Tariff type	Time	Buying price (\$/MWh)	Selling price (\$/MWh)
Tariff 1 (low price)	00:00—06:59	192	180
	07:00—10:59		
Tariff 2 (shoulder price)	16:00—18:59	238	200
	22:00—23:59		
Tariff 3 (peak price)	11:00—15:59	317	260
	19:00—21:59		

Table A.4

Operating cost coefficients of linear demand versus price expression at different tariffs.

Demanders	Tariff 1		Tariff 2		Tariff 3	
	a^{lin}	b^{lin}	a^{lin}	b^{lin}	a^{lin}	b^{lin}
L ₁	0.9	- 0.0028	0.95	- 0.0025	1	- 0.002
L ₂	0.9	- 0.0028	0.95	- 0.0025	1	- 0.002
L ₃	0.9	- 0.0025	0.95	- 0.002	1	- 0.001
L ₄	0.9	- 0.0025	0.95	- 0.002	1	- 0.001
L ₅	0.9	- 0.0025	0.95	- 0.002	1	- 0.001
L ₆	0.9	- 0.0042	0.95	- 0.004	1	- 0.0035
L ₇	0.9	- 0.0042	0.95	- 0.004	1	- 0.0035

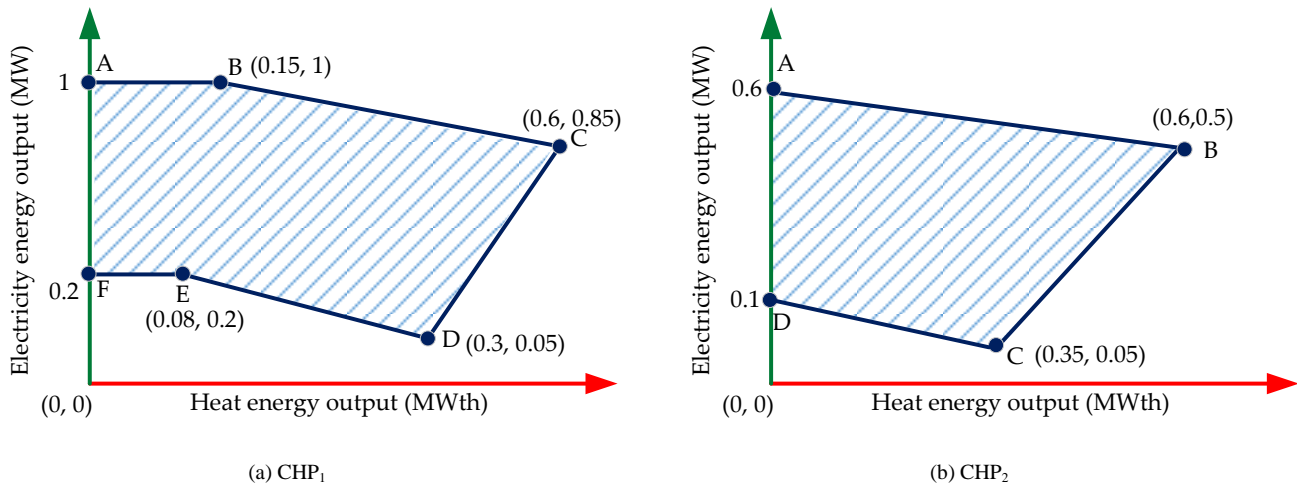


Fig. A.1 Feasible operating regions of two CHP units.

Table A.5

Forecasting results of energy demand and renewable energy outputs under three scenarios.

Demanders or renewables	Energy type	Forecasting results (MW)		
		Scenario 1 (00:00)	Scenario 2 (09:00)	Scenario 3 (14:00)
L ₁	Electricity	0.13	0.38	0.5
	Heat	0.04	0.04	0.03
L ₂	Electricity	0.12	0.33	0.4
	Heat	0.03	0.03	0.03
L ₃	Electricity	0.14	0.42	0.6
	Heat	0.05	0.04	0.04
L ₄	Electricity	0.19	0.38	0.45
	Heat	0.05	0.04	0.03
L ₅	Electricity	0.2	0.44	0.55
	Heat	0.06	0.04	0.04
L ₆	Electricity	0.26	0.4	0.5
	Heat	0.07	0.04	0.04
L ₇	Electricity	0.07	0.18	0.35
	Heat	0.02	0.02	0.02
PV ₁	Electricity	0	0.02	0.1
PV ₂	Electricity	0	0.01	0.1
PV ₃	Electricity	0	0.02	0.1
WT ₁	Electricity	0.28	0.25	0.2
WT ₂	Electricity	0.36	0.32	0.3

References

- [1] Huang AQ, Crow ML, Heydt GT, Zheng JP, Dale SJ. The future renewable electric energy delivery and management system: The energy internet. *Proc IEEE* 2011;99(1):133–48.
- [2] Zhou K, Yang S, Shao Z. Energy internet: The business perspective. *Appl Energy* 2016;178:212–22.
- [3] Palensky P, Widl E, Els Sheikh A. Simulating cyber-physical energy systems: Challenges, tools and methods. *IEEE Trans Syst Man Cybern Syst* 2014;44(3):318–26.
- [4] US National Science Foundation. Cyber-physical systems (CPS). NSF08-611, 2008, <http://www.nsf.gov/pubs/2008/nsf08611/nsf08611.htm>.
- [5] Deng JL, Wang FY, Chen YB, Zhao XY. From industry 4.0 to energy 5.0: Concept and framework of intelligent energy systems. *ACTA Autom Sinica* 2015;41(12):2003-16.
- [6] Zeng J, Yang LT, Lin M, Ning H, Ma J. A survey: Cyber-physical-social systems and their system-level design methodology. *Future Gener Comp Syst* (2016) <https://doi.org/10.1016/j.future.2016.06.034>.
- [7] Wang FY. The emergence of intelligent enterprises: From CPS to CPSS. *IEEE Intell Syst* 2010;25(4):85-8.
- [8] Guzzi F, Neves D, Silva CA. Integration of smart grid mechanisms on microgrids energy modelling. *Energy* 2017;129:321-30.
- [9] Fang X, Ma S, Yang Q, Zhang J. Cooperative energy dispatch for multiple autonomous microgrids with distributed renewable sources and storages. *Energy* 2016;99:48-57.

- [10]Wouters C, Fraga ES, James AM. An energy integrated, multi-microgrid, MILP (mixed-integer linear programming) approach for residential distributed energy system planning–A South Australian case-study. *Energy* 2015;85:30-44.
- [11]Beigvand SD, Abdi H, Scala ML. Hybrid Gravitational Search Algorithm-Particle Swarm Optimization with Time Varying Acceleration Coefficients for large scale CHPED problem. *Energy* 2017;126:841-853.
- [12]Amin SM. Smart grid security, privacy, and resilient architectures: Opportunities and challenges. In: *Proc IEEE power and energy society general meeting, San Diego, CA, USA*. p. 1-2.
- [13]Khan MRB, Jidin R, Pasupuleti J. Multi-agent based distributed control architecture for microgrid energy management and optimization. *Energy Convers Manage* 2016;112:288-307.
- [14]Zhang Z, Chow M Y. Convergence analysis of the incremental cost consensus algorithm under different communication network topologies in a smart grid. *IEEE Trans Power Syst* 2012;27(4):1761-8.
- [15]Yang S, Tan S, Xu JX. Consensus based approach for economic dispatch problem in a smart grid. *IEEE Trans Power Syst* 2013;28(4):4416–26.
- [16]Rahbari-Asr N, Ojha U, Zhang Z, Chow MY. Incremental welfare consensus algorithm for cooperative distributed generation/demand response in smart grid. *IEEE Trans Smart Grid* 2014;5(6):2836-45.
- [17]Chen G, Zhao Z. Delay Effects on consensus-based distributed economic dispatch algorithm in microgrid. *IEEE Trans Power Syst* (2017) doi: 10.1109/TPWRS.2017.2702179.
- [18]Dall'Anese E, Zhu H, Giannakis GB. Distributed optimal power flow for smart microgrids. *IEEE Trans Smart Grid* 2013;4(3):1464-75.
- [19]Liu N, Wang J, Wang L. Distributed energy management for interconnected operation of combined heat and power-based microgrids with demand response. *J Mod Power Syst Clean Energy* 2017;5(3):478-88.
- [20]Saad W, Han Z, Poor HV, Basar T. Game-theoretic methods for the smart grid: An overview of microgrid systems, demand-side management, and smart grid communications. *IEEE Signal Processing Mag* 2012;29(5):86-105.
- [21]Ma L, Liu N, Zhang J, Tushar W, Yuen C. Energy management for joint operation of CHP and PV prosumers inside a grid-connected microgrid: A game theoretic approach. *IEEE Trans Ind Inf* 2016;2(5):1930-42.
- [22]Dehghanpour K, Nehrir H. Real-time multiobjective microgrid power management using distributed optimization in an agent-based bargaining framework. *IEEE Trans Smart Grid* (2017) doi:10.1109/TSG.2017.2708686.
- [23]Subbaraj P, Rengaraj R, Salivahanan S. Enhancement of combined heat and power economic dispatch using self adaptive real-coded genetic algorithm. *Appl Energy* 2009;86(6):915-21.
- [24]Greenwald A, Hall K. Correlated-Q learning. in *Proc 20th Int Conf Mach Learn (ICML-03)*, Washington, DC, USA, Aug. 21–24, 2003:242-9.

- [25] Hetzer J, Yu DC, Bhattarai K. An economic dispatch model incorporating wind power. *IEEE Trans Energy Convers* 2008;23(2):603-11.
- [26] Brini S, Abdallah HH, Ouali A. Economic dispatch for power system included wind and solar thermal energy. *Leonardo J Sci* 2009;14:204-20.
- [27] Aghaei J, Alizadeh MI. Multi-objective self-scheduling of CHP (combined heat and power)-based microgrids considering demand response programs and ESSs (energy storage systems). *Energy* 2013;55:1044-54.
- [28] Karki S, Kulkarni M, Mann MD, Salehfar H. Efficiency improvements through combined heat and power for on-site distributed generation technologies. *Cogener Distrib Gener J* 2007;22:19-34.
- [29] Piperagkas GS, Anastasiadis AG, Hatziaargyriou ND. Stochastic PSO-based heat and power dispatch under environmental constraints incorporating CHP and wind power units. *Electr Power Syst Res* 2011;81(1):209-18.
- [30] Yousefi S, Moghaddam MP, Majd VJ. Optimal real time pricing in an agent-based retail market using a comprehensive demand response model. *Energy* 2011;36(9):5716-27.
- [31] Wang FY, Zhang J, Wei Q, Li L. PDP: Parallel dynamic programming. *IEEE/CAA J Autom Sinica* 2017;4(1):1-5.
- [32] Yu T, Zhang XS, Zhou B, Chan KW. Hierarchical correlated Q-learning for multi-layer optimal generation command dispatch. *Int J Electr Power Energy Syst* 2016;78:1-12.
- [33] Bianchi RAC, Celiberto LA, Santos PE, Matsuura JP, Mantaras RL. Transferring knowledge as heuristics in reinforcement learning: A case-based approach. *Artif Intell* 2015;226:102-21.
- [34] Godsil C, Royle G. *Algebraic graph theory*. New York: Springer-Verlag; 2001.
- [35] Moreau L. Stability of multiagent systems with time-dependent communication links. *IEEE Trans Autom Control* 2005;50(2):169-82.
- [36] Yan X, Yang W, Shi H. A group search optimization based on improved small world and its application on neural network training in ammonia synthesis. *Neurocomputing* 2012;97:94-107.
- [37] Iba K. Reactive power optimization by genetic algorithm. *IEEE Trans Power Syst* 1994;9(2):685-92.
- [38] Clerc M, Kennedy J. The particle swarm: Explosion, stability, and convergence in a multidimensional complex space. *IEEE Trans Evol Comput* 2002;6(1):58-73.
- [39] Secui DC. The chaotic global best artificial bee colony algorithm for the multi-area economic/emission dispatch. *Energy* 2015;93:2518-45.
- [40] He S, Wu QH, Saunders JR. Group search optimizer: An optimization algorithm inspired by animal searching behavior. *IEEE Trans Evol Comput* 2009;13(5):973-90.